



OPEN ACCESS

EDITED BY

Sébastien Bontemps-Gallo,
Institut Pasteur de Lille, Univ. Lille, France

REVIEWED BY

Alexandra E. Purdy,
Amherst College, United States
Rishita Chourashi,
University of Maryland, United States

*CORRESPONDENCE

Jian Huang
✉ 81537648@qq.com
Xun Min
✉ minxunzmu@163.com

†These authors have contributed equally to this work

RECEIVED 19 August 2024

ACCEPTED 14 October 2024

PUBLISHED 01 November 2024

CITATION

Zhao J, Huang X, Li Q, Ren F, Hu H, Yuan J, Wang K, Hu Y, Huang J and Min X (2024) DegS regulates the aerobic metabolism of *Vibrio cholerae* via the ArcA-isocitrate dehydrogenase pathway for growth and intestinal colonization. *Front. Cell. Infect. Microbiol.* 14:1482919. doi: 10.3389/fcimb.2024.1482919

COPYRIGHT

© 2024 Zhao, Huang, Li, Ren, Hu, Yuan, Wang, Hu, Huang and Min. This is an open-access article distributed under the terms of the [Creative Commons Attribution License \(CC BY\)](https://creativecommons.org/licenses/by/4.0/). The use, distribution or reproduction in other forums is permitted, provided the original author(s) and the copyright owner(s) are credited and that the original publication in this journal is cited, in accordance with accepted academic practice. No use, distribution or reproduction is permitted which does not comply with these terms.

DegS regulates the aerobic metabolism of *Vibrio cholerae* via the ArcA-isocitrate dehydrogenase pathway for growth and intestinal colonization

Jiajun Zhao^{1,2†}, Xiaoyu Huang^{1,2†}, Qingqun Li^{3†}, Fangyu Ren^{1,2}, Huaqin Hu^{1,2}, Jianbo Yuan^{1,2}, Kaiying Wang^{1,2}, Yuanqin Hu^{1,2}, Jian Huang^{1,2*} and Xun Min^{1,2*}

¹Department of Laboratory Medicine, Affiliated Hospital of Zunyi Medical University, Zunyi, Guizhou, China, ²School of Laboratory Medicine, Zunyi Medical University, Zunyi, Guizhou, China,

³Department of Laboratory Medicine, Kweichow Moutai Hospital, Zunyi, Guizhou, China

Aerobic respiration is the key driver of *Vibrio cholerae* proliferation and infection. Our previous transcriptome results suggested that *degS* knockout downregulates a few genes involved in NADH and ATP synthesis in the aerobic respiratory pathway. In this study, non-targeted metabolomics results showed that the differential metabolites affected by *degS* knockout were associated with aerobic respiration. Further results suggested that the key products of aerobic respiration, NADH and ATP, were reduced upon *degS* deletion and were not dependent on the classical σ^E pathway. The two-component system response factor aerobic respiration control A (ArcA) is involved in regulating NADH and ATP levels. qRT-PCR demonstrated that DegS negatively regulates the transcription of the *arcA* gene, which negatively regulates the expression of isocitrate dehydrogenase (ICDH), a key rate-limiting enzyme of the tricarboxylic acid cycle. NADH and ATP levels were partially restored with the knockout of the *arcA* gene in the $\Delta degS$ strain, while levels were partially restored with overexpression of ICDH in the $\Delta degS$ strain. In a growth experiment, compared to the $\Delta degS$ strain, the growth rates of $\Delta degS \Delta arcA$ and $\Delta degS$ -overexpressed *icdh* strains ($\Delta degS+icdh$) were partially restored during the logarithmic growth period. Colonization of the intestines of suckling mice showed a significant reduction in the colonizing ability of the $\Delta degS$ strain, similar colonizing ability of the $\Delta degS::degS$ strain and the wild-type strain, and a partial recovery of the colonizing ability of the $\Delta degS+icdh$ strain. Overall, these findings suggest that the DegS protease regulates the expression of ICDH through ArcA, thereby affecting the NADH and ATP levels of *V. cholerae* and its growth and intestinal colonization ability.

KEYWORDS

Vibrio cholerae, DegS protease, aerobic metabolism, growth, intestinal colonization

Introduction

Vibrio cholerae is a facultative anaerobic bacterium capable of both aerobic and anaerobic respiration (Reen et al., 2006). Bacteria produce chemical energy through aerobic-mediated energy metabolism, which is stored in the form of ATP to power the cellular processes required for growth. Both aerobic and anaerobic metabolisms are essential for the growth of *V. cholerae* *in vivo* (Bueno et al., 2020; Van Alst and DiRita, 2020). Aerobic respiration acts as a powerful driver of replication during infection with the *V. cholerae* gastrointestinal pathogen (Harris et al., 2012). In one study, *V. cholerae* incapable of aerobic respiration was strongly attenuated (10^5 times) in young mice, whereas strains lacking anaerobic respiration showed no colonization defects (Van Alst et al., 2022). In a suckling mouse model, a related study reported that defects in the *pyruvate dehydrogenase* aerobic respiration gene of *V. cholerae* resulted in a significant decrease in colonization rates (Van Alst and DiRita, 2020). *In vitro*, *V. cholerae* undergoes aerobic respiration, which produces the metabolic intermediates succinate and pyruvate, resulting in increased motility (Kiiyukia et al., 1993). In addition, aerobic respiration promotes the transcription of the virulence factor *toxT* in *V. cholerae* during pathogenesis. Consequently, aerobic respiration plays a vital role in the pathogenicity of *V. cholerae* (Medrano et al., 1999; Fan et al., 2014). Concerning the control of cholera, it would be desirable to identify mechanisms that regulate aerobic respiration in *V. cholerae* and establish methods that can attenuate its effects.

The tricarboxylic acid (TCA) cycle is an important intermediate link in aerobic respiration and is regarded as the energy-generating engine of aerobic respiration for ATP synthesis. This function connects glycolysis and the electron transport chain and is a central part of cellular energy metabolism (MacLean et al., 2023). Aerobic respiration control A (ArcA) is a response factor in the two-component Arc system that acts as a global inhibitor of the aerobic respiratory pathway (particularly the TCA cycle), thereby promoting the bacterial fermentation pathway (Wang et al., 2018). Recently, a study demonstrated that overexpression of ArcA under aerobic conditions leads to downregulation of the respiratory pathway in *E. coli* (Basan et al., 2017). Hence, it is important to investigate the regulatory mechanisms of aerobic respiration in *V. cholerae* in terms of the global inhibitors of the TCA cycle.

Serine protease DegS is commonly recognized as an initiator of the σ^E (*rpoE*) stress response pathway (de Regt et al., 2015), which affects *V. cholerae* motility, chemotaxis and antioxidant capacity (Wang et al., 2023a; Zou et al., 2023). Our previous results by RNA sequencing (RNA-seq) showed that the knockout of *degS* resulted in the downregulation of genes associated with aerobic respiration, which are focused on the TCA cycle (Huang et al., 2019), but the mechanisms involved are not clear. In the current study, metabolomics analysis revealed that the differential metabolites of the $\Delta degS$ mutant were mainly enriched in purine metabolism and glutathione metabolism associated with aerobic respiration, suggesting that DegS may regulate aerobic respiration in *V.*

cholerae. This study investigated the influence of DegS on the key products of aerobic respiration, NADH, and ATP. Our results suggest that DegS affects isocitrate dehydrogenase (ICDH) expression through the regulation of ArcA, thereby affecting aerobic respiration in *V. cholerae*, which in turn affects NADH and ATP production.

Materials and methods

Bacterial strains and growth conditions

Non-O1/non-O139 *V. cholerae* HN375 from the China Center for Type Culture Collection (CCTCCAB209168) was used as the wild-type (WT) strain (Luo et al., 2011). Cloning was carried out using *Escherichia coli* DH5 and DH5- λ pir, and conjugation were carried out using WM3064. Each strain was grown on Luria-Bertani (LB) medium at 37°C until the stationary phase was achieved unless otherwise indicated. The culture medium was modified by adding 0.1% arabinose and 100 g/mL ampicillin depending on the situation. Details of all plasmids and strains used are presented in [Supplementary Table 1](#).

DNA manipulations and genetic techniques

From the WT HN375 strain, deletion mutants were constructed with pWM91, a suicide plasmid (Wu et al., 2015). A list of the primers used can be found in [Supplementary Table 2](#). To construct complementary mutants, the entire *arcA* encoding region by cloning into the pBAD24 plasmid vector, which was then transformed into $\Delta degS \Delta arcA$ by electroporation to obtain $\Delta degS \Delta arcA::arcA$. A similar method was used to construct $\Delta degS$ -overexpressed *icdh* strains ($\Delta degS+icdh$). As previously described, we used the pBAD24-*arcA* plasmid as a template and constructed a point mutation in D54E of *arcA* using site-directed mutagenesis (Fisher and Pei, 1997). The pBAD24-*arcA*^{D54E} plasmid vector was then transformed into $\Delta degS \Delta arcA$ by electroporation to obtain $\Delta degS \Delta arcA::arcA^{D54E}$. The complement and overexpression strains were grown in LB liquid medium with 0.1% arabinose for gene expression induction.

Untargeted metabolomic analysis

The WT and $\Delta degS$ strains were added into sterile LB liquid medium and shaken at 220 rpm and incubated at 37°C until the logarithmic growth phase (optical density at 600 nm [OD₆₀₀] = 0.6). Both cultures were centrifuged at 10,000 g during 10 min at 4°C. After collection, the pellets were washed twice with 50 mM PBS, and used for untargeted metabolomic analysis. This analysis was performed by Biotech-Pack Scientific Co., Ltd. (Beijing, China). The Analysis Base File (ABF) converter software was used to convert the liquid chromatography-mass spectrometry (LC-MS)

raw data into the ABF format (Zhang et al., 2021). The ABF format file was imported into MS-DIAL 4.10 software for preprocessing (D'Oria et al., 2022), including peak extraction, noise removal, inverse convolution, and alignment. The three-dimensional (3D) data matrix was exported in the CSV format (raw data matrix). Finally, the extracted peak information was searched against the MassBank, Respect, and Global Natural Product Social Molecular Networking (GNPS), for a full library comparison.

Quantitative RT-PCR

All strains were grown to the stationary phase ($OD_{600} = 1.2$) in an LB liquid medium. Bacterial cultures were collected via centrifugation at 8000 rpm for 5 min. Total RNA was extracted with TRIzol reagent and reverse-transcribed into cDNA. qRT-PCR was performed using the TB Green Premix Ex TaqII (TaKaRa Bio, Shiga, Japan) (Huang et al., 2019). The $2^{-\Delta\Delta Ct}$ method was used to calculate mRNA levels relative to each other (Livak and Schmittgen, 2001). For each qRT-PCR, two independent experiments were performed, each with three technical replicates.

Assay of bacterial NADH levels

To examine the NADH levels of bacteria grown in LB liquid medium or M9 liquid medium (containing 0.4% glucose) to stationary phase ($OD_{600} = 1.2$), the concentration of bacteria was adjusted to approximately 1×10^8 CFU/mL. The bacteria were ultrasonically lysed. NADH levels were measured using the Amplitude™ Colorimetric NADH Assay Kit (AAT Bioquest, Pleasanton, CA, USA). Briefly, equal volumes of bacterial suspension and Amplitude™ Colorimetric NADH Assay Kit working solution were mixed and dispensed in wells of a clear 96-well plate, followed by incubation at 26°C for 15 min to 2 h. Read the absorbance at 460 nm using an enzyme marker and construct a standard curve using the kit's NADH standard (Xia et al., 2021). The experiment was repeated three times.

Bacterial ATP levels assay

ATP levels were determined using an ATP Assay Kit (Beyotime, Shanghai, China) following the manufacturer's instructions. Briefly, the bacteria were cultured to stationary phase in LB liquid medium or M9 liquid medium (containing 0.4% glucose) and the bacterial concentration was adjusted to 1×10^8 CFU/mL. The bacteria were ultrasonically lysed. Equal volumes of the bacterial suspension and the working solution in the ATP reagent were mixed in a black opaque 96-well plate and incubated at 26°C for 5 min (Janet-Maitre et al., 2023). Luminescence was detected using a multifunctional enzyme labeler (Thermo Fisher Scientific Inc, Waltham, MA, USA). A standard curve was plotted using the standards provided in the kit. The experiment was repeated three times.

Recombinant protein expression, purification, and preparation of polyclonal antisera

The His-tagged recombinant ArcA protein was constructed as previously described (Wang et al., 2023b). Briefly, primers were used to amplify the full-length ArcA-encoded open reading frames. The PCR product was ligated into the pET28a vector and transformed into *E. coli* BL21 (DE3). Transformed bacteria expressing ArcA were grown to $OD_{600} = 0.6$ at 37°C and induced with 0.5 mM isopropyl β -D-1-thiogalactopyranoside (IPTG) at 18°C for 16 h in LB liquid medium. Recombinant proteins labeled with His were purified by nickel-nitrilotriacetic acid affinity chromatography. Eight 6-week-old CD1 female mice, provided by the animal center of Zunyi Medical University (Zunyi, China), were housed in a specific pathogen-free environment and used to prepare anti-ArcA serum for western blot analysis. Mice were subcutaneously inoculated with 30 μ g of recombinant ArcA on days 0, 14, and 28, along with the same volume of aluminum adjuvant. Anti-ArcA antiserum was prepared from blood collected 2 weeks after the last immunization.

Western blot

All strains were grown to stationary phase ($OD_{600} = 1.2$) in an LB liquid medium. To prepare whole bacterial proteins, the culture was subjected to centrifugation, resulting in the separation of a supernatant layer. The precipitate was resuspended with 100 μ L of distilled deionized water and 25 μ L of 5 \times sodium dodecyl sulfate-polyacrylamide gel electrophoresis (SDS-PAGE) protein sampling buffer was added and boiled. The bacterial proteins were resolved by SDS-PAGE and transferred to a polyvinylidene fluoride membrane. After blocking, the membrane was incubated with a primary antibody (anti-ArcA serum at a dilution of 1:1000, prepared in our laboratory) overnight at 4°C. The membrane was incubated with a 1:5000 dilution of horseradish peroxidase-conjugated sheep anti-mouse IgG as a secondary antibody for 2 h after three washes with 1 \times Tris-buffered saline containing 0.1% Tween-20 (TBST). Finally, the membrane was washed three times with TBST, and color developed after the addition of chemiluminescent reagents (Epizyme Biomedical Technology Co. Ltd, Shanghai, China). The experiment was repeated three times.

Bacterial growth curves

Growth curves were generated as described previously (Kovač et al., 2021) with certain modifications. Briefly, the bacteria were cultured in LB liquid medium at 37°C until the stationary phase ($OD_{600} = 1.2$). Aliquots of the culture were inoculated (1:500 v/v) into M9 liquid medium containing 0.4% glucose and incubated at 37°C with shaking at 200 rpm. Measurements were taken hourly for absorbance at 600 nm. The experiment was repeated three times.

Suckling mouse colonization assay

Six-day-old CD1 suckling mice which were randomized into the experimental and control groups ($n = 8$ per group). All animal experiments were approved by the Ethics Committee of Zunyi Medical University (No. ZMU21-2301-069). All strains were grown at 37°C to stationary phase ($OD_{600} = 1.2$), and the bacteria were collected by centrifugation at $1,200 \times g$ for 5 min. The bacterial concentration was adjusted to 1×10^7 CFU/mL with PBS. Each suckling mouse in the experimental group was gavaged with 50 μ L of the bacterial suspension. The same volume of $1 \times$ PBS was used in the negative control. In the 18th hour following gavage, mice were euthanized. The small intestinal tissue was subsequently dissected, weighed, and homogenized (Zou et al., 2023). After 100-fold dilution of this preparation, 100 μ L aliquots were added to 0.5 mg/L gentamicin agar plates, and the colonies were counted after 18 h of incubation at 37°C. The final results are presented as the logarithm CFU/g.

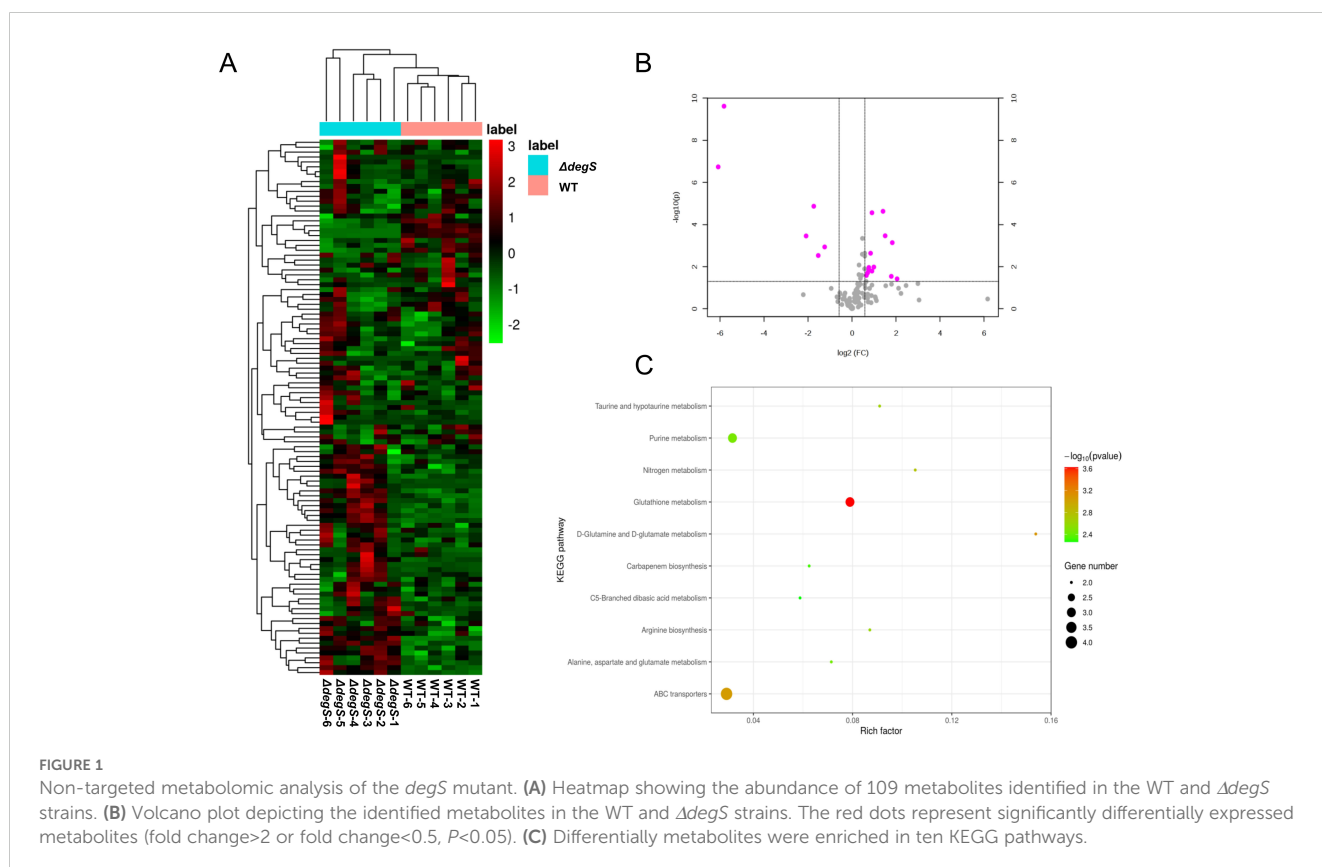
Statistical analyses

Data are expressed as mean \pm standard deviation. Non-paired two-tailed t-tests were used to analyze differences between two groups, and a one-way analysis of variance was used to analyze differences between multiple groups. SPSS version 29.0 (IBM Corp., Armonk, NY, USA) was used for the analyses. $P < 0.05$ indicated statistical significance.

Results

Non-targeted metabolomic analysis of the *degS* mutant

Our previous RNA-seq data suggested that the knockout of *degS* results in the downregulation of genes related to the TCA cycle of the aerobic respiration pathway (Huang et al., 2019). The finding implies that DegS may affect aerobic respiration in *V. cholerae*. To further test this hypothesis, we conducted untargeted metabolomics on *degS* knockout mutants ($\Delta degS$). The analysis identified a total of 109 metabolites (Figure 1A; Supplementary Table 3). Significantly ($P < 0.05$) differentially expressed metabolites were screened according to fold changes > 2 or < 0.5 . A combination of multidimensional and unidimensional analyses identified 19 significantly differentially expressed metabolites (Table 1). One-dimensional statistical analyses were performed using multiplicity and t-tests. The resulting data were plotted as volcano plots (Figure 1B). Kyoto Encyclopedia of Genes and Genomes (KEGG) pathway enrichment analysis of enriched genes mainly revealed genes involved in purine and glutathione metabolism (Figure 1C). Glutathione metabolism is an important component of aerobic respiration and provides important redox buffers (Lushchak, 2012; Hatem et al., 2014). Purine metabolism provides purine nucleotides that are essential for ATP production from aerobic respiration (Gessner et al., 2023). These findings indicate that DegS has an impact on aerobic respiration in *V. cholerae*.



DegS positively affects NADH and ATP levels in *V. cholerae*

Given the transcriptome and metabolome results, we hypothesized that DegS may affect the production of the aerobic respiration pathway products NADH and ATP. To test this hypothesis, we determined the levels of NADH in WT and $\Delta degS$ strains. The NADH levels of the WT strain were approximately twice as high as those of the $\Delta degS$ mutants, whereas the NADH levels of the complemented strain $\Delta degS::degS$ were able to restore NADH levels close to those of the WT strain (Figure 2A). The pBAD24 null plasmid was unable to recover the NADH levels of $\Delta degS$. Subsequently, we investigated ATP levels in the above strains, which is the final energy product of the aerobic respiration pathway. The ATP level of the WT strain was approximately thrice that of $\Delta degS$, whereas the ATP levels of $\Delta degS::degS$ were partially restored, with no restoration using the pBAD24 empty plasmid (Figure 2B). The above data suggest that DegS influences positively NADH and ATP levels in *V. cholerae*.

DegS positively affects NADH and ATP levels in *V. cholerae* independent of σ^E

DegS regulates stress response and motility through σ^E and DegS deficiency significantly reduces σ^E activity (Ades et al., 1999). To investigate whether DegS affects *V. cholerae* NADH and ATP levels via σ^E , we first examined the transcript levels of *rpoE*. The qRT-PCR results showed that the *rpoE* gene transcript level in the WT strain was approximately four times higher than that of $\Delta degS$, while the transcript level of the *rpoE* gene in $\Delta degS::degS$ was almost the same as that of the WT strain (Figure 3A). Next, we performed experiments for the detection of NADH and ATP levels using the *rpoE* deletion mutant ($\Delta rpoE$) and corresponding complemented strain ($\Delta rpoE::rpoE$). The NADH level of the $\Delta rpoE$ mutant was not statistically different from the WT and $\Delta rpoE::rpoE$ strains (Figure 3B). The ATP levels of the *rpoE* mutation did not differ from that of the WT and $\Delta rpoE::rpoE$ strains (Figure 3C). We used qRT-PCR to screen for changes in the expression of some aerobic respiratory genes in different strains, and the expression levels of genes encoding type I glyceraldehyde-3-phosphate dehydrogenase

TABLE 1 Significantly differentially expressed metabolites of WT and $\Delta degS$ strains.

Compounds	Log2 Fold Change ($\Delta degS/WT$)	$-\log_{10}(P \text{ value})$
9-methoxy-7-[4-[(2S,3R,4S,5S,6R)-3,4,5-trihydroxy-6-(hydroxymethyl)oxan-2-yl]oxyphenyl]-[1,3]dioxolo[4,5-g]chromen-8-one	-5.82	6.74
(4R)-3-methylidene-4-[(E)-3-methyl-4-(4-methyl-5-oxoxolan-2-yl)but-2-enyl]oxolan-2-one	-6.08	4.87
(E)-8-(4-hydroxy-6-methoxy-7-methyl-3-oxo-1H-2-benzofuran-5-yl)-2,6-dimethyloct-6-enoic acid	-1.74	4.63
(2S,6R,8aS)-6-(2-hydroxypropan-2-yl)-8a-methyl-4-methylidene-1,2,3,4a,5,6,7,8-octahydronaphthalen-2-ol-	1.41	4.56
Leupeptin	0.90	3.47
L-5-Oxoproline	1.50	3.46
Lenacil	-2.09	3.14
Falcarindiol	1.83	2.94
Glycine-Betaine	-1.25	2.64
DL-Coniine	0.84	2.53
Glycerophosphate(2)	-1.54	1.98
5-pentyl-2-furannonanoic acid	0.99	1.96
Tectorigenin	0.76	1.87
2-[2-(3,4-dimethoxyphenyl)ethyl]-4-methoxy-2,3-dihydropyran-6-one	0.76	1.79
Norharman	0.90	1.71
8-Prenylnaringenin	0.71	1.59
(3S)-5-[(1S,8aR)-2,5,5,8a-tetramethyl-4-oxo-4a,6,7,8-tetrahydro-1H-naphthalen-1-yl]-3-methylpentanoic acid	0.65	1.54
5-(1,2,4a,5-tetramethyl-7-oxo-3,4,8,8a-tetrahydro-2H-naphthalen-1-yl)-3-methylpentanoic acid	1.78	1.42
2'-Deoxyadenosine	2.05	4.87

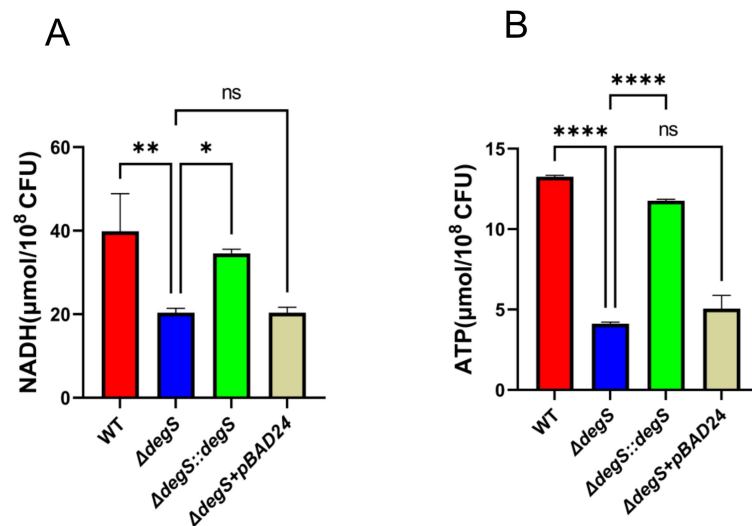


FIGURE 2 DegS positively affects NADH and ATP levels in *V. cholerae*. **(A)** Detection of NADH levels in wild type (WT), $\Delta degS$, $\Delta degS::degS$, and $\Delta degS + pBAD24$. **(B)** Assay of ATP levels in each strain. Data are expressed as the mean and standard deviation of biological replicates ($n = 3$). One-way analysis of variance (ANOVA) was employed for the analysis of the data. *, $P < 0.05$; **, $P < 0.01$; ****, $P < 0.0001$; ns indicates no statistical significance.

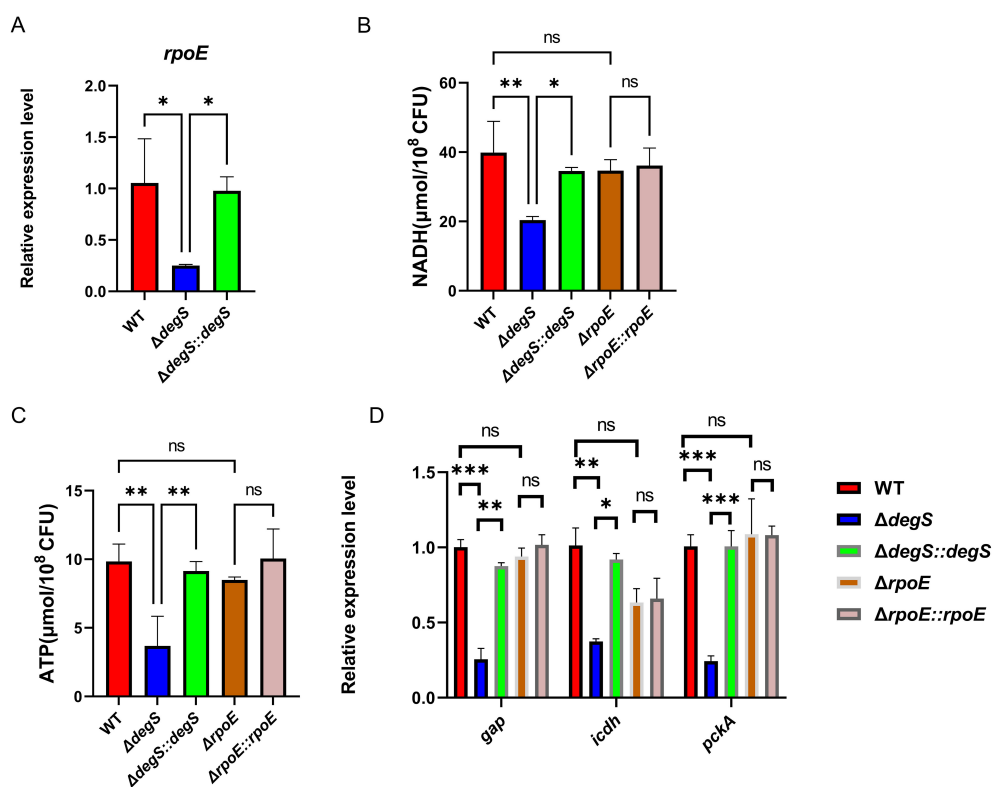


FIGURE 3 DegS positively affects NADH and ATP levels in *V. cholerae* independent of σ^E . **(A)** The mRNA levels of *rpoE* in the WT, $\Delta degS$, and $\Delta degS::degS$. **(B, C)** Detection of NADH **(B)** and ATP **(C)** levels in WT, $\Delta degS$, $\Delta degS::degS$, $\Delta rpoE$, and $\Delta rpoE::rpoE$. **(D)** The mRNA levels of aerobic respiration-related genes in each strain. Analyses were performed using the one-way ANOVA statistical method. The data are presented as the mean and standard deviation of each of three biological replicates. ($n = 3$). *, $P < 0.05$; **, $P < 0.01$; ***, $P < 0.001$; ns indicates no statistical significance.

(GAP), isocitrate dehydrogenase (ICDH), and phosphoenolpyruvate carboxykinase (PckA) were significantly reduced in the $\Delta degS$ mutant as compared with the WT strain (Figure 3D). However, the expression of the above genes did not change after *rpoE* knockout. These results indicate that DegS positively affects NADH and ATP levels in *V. cholerae* independent of σ^E .

Effect of DegS on NADH and ATP levels in *V. cholerae* involves ArcA

In *S. typhimurium*, ArcA may negatively regulate ATP and NADH levels by inhibiting gene transcription levels of the pyruvate dehydrogenase complex (PDH) in the TCA cycle (Morales et al., 2013). Using qRT-PCR, we observed that the transcript level of *arcA*

in $\Delta degS$ was approximately six times higher than that of the WT strain (Figure 4A), suggesting that DegS is a negative regulator of ArcA. Therefore, we hypothesized that DegS influences the NADH and ATP levels in *V. cholerae* through ArcA. To assess the hypothesis, we constructed $\Delta degS \Delta arcA$ and $\Delta degS \Delta arcA::arcA$ and measured the levels of NADH and ATP. Both levels in $\Delta degS \Delta arcA$ could be partially restored compared to $\Delta degS$ (Figures 4B, C). Next, we detected the expression level of ArcA protein in each strain. ArcA protein expression was almost the same in WT strains, $\Delta degS$, and $\Delta degS::degS$ (Figure 4D). ArcA is a response factor in a two-component system that can activate downstream genes in a phosphorylated form. Meanwhile, in *E. coli*, ArcA is an important inhibitor, and its phosphorylated form directly inhibits the expression of some genes in the TCA cycle, such as citrate synthase (GltA) and malate dehydrogenase (MDH) (Park

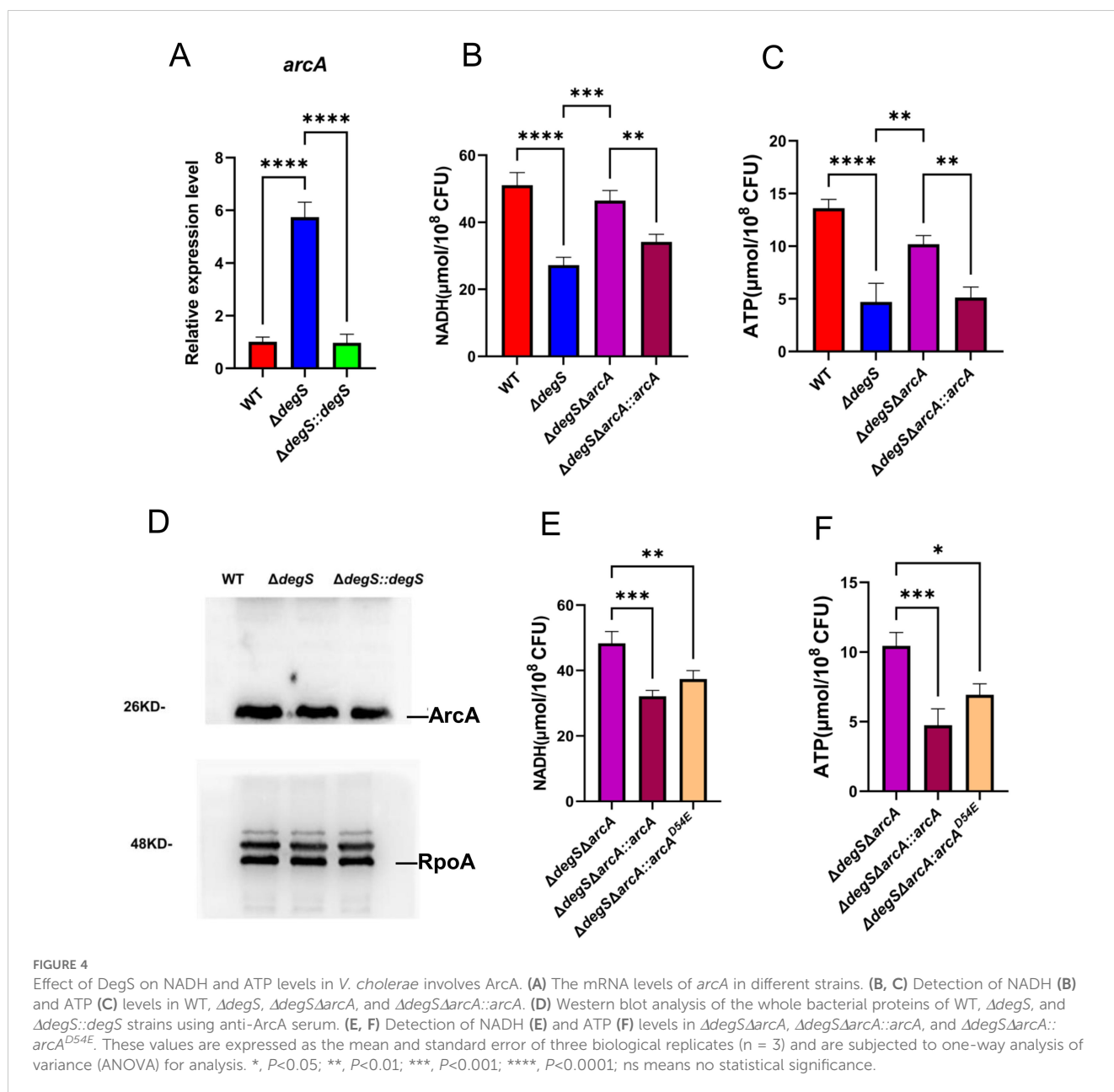


FIGURE 4

Effect of DegS on NADH and ATP levels in *V. cholerae* involves ArcA. (A) The mRNA levels of *arcA* in different strains. (B, C) Detection of NADH (B) and ATP (C) levels in WT, $\Delta degS$, $\Delta degS \Delta arcA$, and $\Delta degS \Delta arcA::arcA$. (D) Western blot analysis of the whole bacterial proteins of WT, $\Delta degS$, and $\Delta degS::degS$ strains using anti-ArcA serum. (E, F) Detection of NADH (E) and ATP (F) levels in $\Delta degS \Delta arcA$, $\Delta degS \Delta arcA::arcA$, and $\Delta degS \Delta arcA::arcA^{D54E}$. These values are expressed as the mean and standard error of three biological replicates (n = 3) and are subjected to one-way analysis of variance (ANOVA) for analysis. *, $P < 0.05$; **, $P < 0.01$; ***, $P < 0.001$; ****, $P < 0.0001$; ns means no statistical significance.

et al., 2013). Therefore, we speculated whether its phosphorylation modifications are involved in this regulatory process. Next, we constructed a point mutation model ($\Delta degS \Delta arcA::arcA^{D54E}$) to mimic dephosphorylation (Jeon et al., 2001) to explore whether ArcA phosphorylation is associated with DegS affecting NADH and ATP levels in *V. cholerae*. Both NADH and ATP levels were decreased in the $\Delta degS \Delta arcA::arcA^{D54E}$ strain compared to the $\Delta degS \Delta arcA$ strain. The $\Delta degS \Delta arcA::arcA^{D54E}$ strain had a smaller decrease in NADH and ATP levels than the $\Delta degS \Delta arcA::arcA$ strain (Figures 4E, F). These results suggest that DegS affects NADH and ATP levels, which are partially dependent on ArcA phosphorylation.

Effect of DegS on NADH and ATP levels in *V. cholerae* involved in expressing ICDH

ICDH is a key rate-limiting enzyme of the TCA cycle; the knockdown of ICDH leads to a decrease in bacterial NADH and ATP levels (Kabir and Shimizu, 2004a). Our qRT-PCR results revealed that the transcription level of *icdh* in $\Delta degS$ strains was approximately five times lower than that of WT strains and that the transcriptional level of *icdh* was recovered in part in the $\Delta degS \Delta arcA$ strain (Figure 5A). These findings suggest that DegS may control the transcription of *icdh* through the ArcA pathway. To determine whether ICDH is involved in regulating *V. cholerae* NADH and ATP levels in DegS, we overexpressed ICDH based on the $\Delta degS$ strain and measured NADH and ATP levels. Both levels were partially restored in the $\Delta degS+icdh$ strain, but not to the level of the WT strain (Figures 5B, C). Collectively, these results suggest that DegS is required for high levels of ATP and NADH because it indirectly increases ICDH expression.

DegS affects the growth of *V. cholerae* through the ArcA-ICDH pathway

Many enzymes and metabolites associated with bacterial energy metabolism have direct regulatory roles in bacterial growth (Kabir and Shimizu, 2004a; Weart et al., 2007; Hill et al., 2013; Sperber and Herman, 2017). Our experiments showed that DegS affects ATP and NADH levels in *V. cholerae* through the ArcA-ICDH signaling pathway. To confirm whether DegS affects growth in *V. cholerae* through this pathway, we conducted growth curve experiments in the M9 medium. The growth rate of the $\Delta degS$ strain was lower than that of the WT strain during the logarithmic growth phase (Figure 6A). Compared to the $\Delta degS$ strain, the $\Delta degS \Delta arcA$ strain grew faster during the logarithmic growth period. The $\Delta degS+icdh$ strain had a faster growth rate than the $\Delta degS$ strain during the logarithmic growth phase (Figure 6B). Concurrently, the trends of NADH and ATP levels of the $\Delta degS \Delta arcA$ strain and the $\Delta degS+icdh$ strain in M9 medium corresponded to the trends of their growth rates in the logarithmic growth phase (Figures 6C, D). These evidences demonstrate that DegS affects the growth of *V. cholerae* through the ArcA-ICDH pathway.

DegS affects *V. cholerae* intestinal colonization

Inhibition of NADH and ATP production in bacteria affects their colonization (Jones et al., 2007; Schurig-Briccio et al., 2020). To examine whether the regulation of *V. cholerae* NADH and ATP levels mediated by DegS is critical for bacterial colonization, we used a suckling mouse model of intestinal colonization. The *in vivo* results showed that compared with the WT strain, the colonization

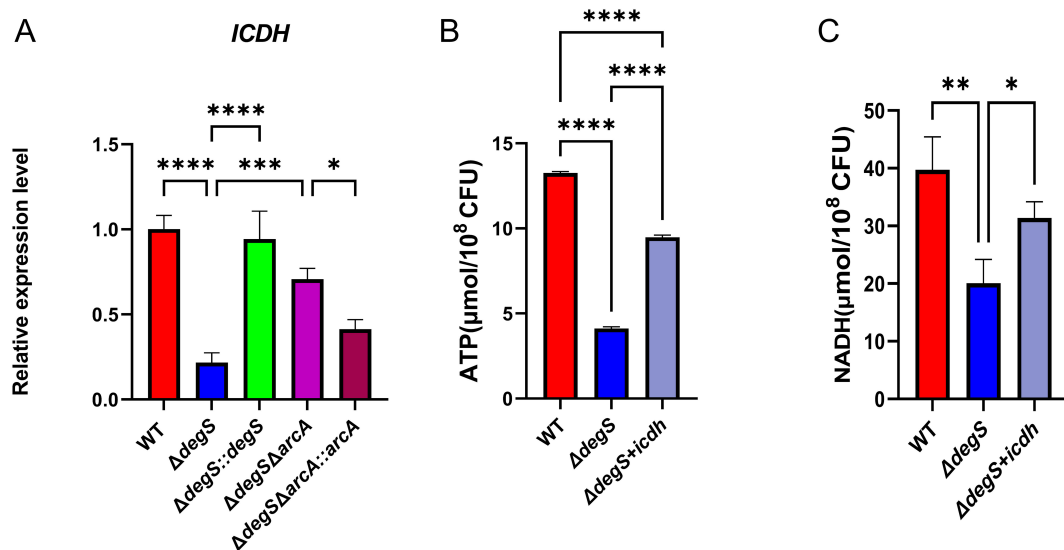


FIGURE 5
Effect of DegS on NADH and ATP levels in *V. cholerae* involved in the expression of ICDH. (A) The mRNA levels of *icdh* in WT, $\Delta degS$, $\Delta degS::degS$, $\Delta degS \Delta arcA$, and $\Delta degS \Delta arcA::arcA$ strains. (B, C) Detection of ATP (B) and NADH (C) levels in WT, $\Delta degS$, and $\Delta degS+icdh$. Data are expressed as mean and standard deviation of three biological replicates ($n = 3$) and were analyzed using one-way ANOVA. *, $P < 0.05$; **, $P < 0.01$; ***, $P < 0.001$; ****, $P < 0.0001$.

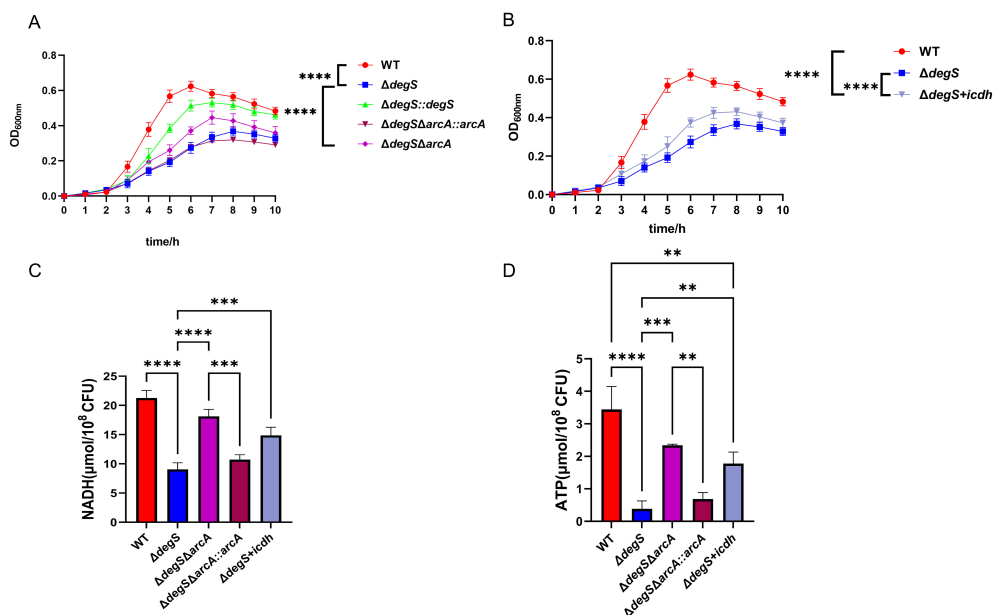


FIGURE 6

DegS affects the growth of *V. cholerae* through the ArcA-ICDH pathway. (A, B) Growth curves of WT, $\Delta degS$, $\Delta degS::degS$, $\Delta degS\Delta arcA$, $\Delta degS\Delta arcA::arcA$, and $\Delta degS+icdh$ strains in M9 medium with 0.4% glucose added at 37°C. (C, D) Detection of NADH (C) and ATP (D) levels of WT, $\Delta degS$, $\Delta degS\Delta arcA$, $\Delta degS\Delta arcA::arcA$, and $\Delta degS+icdh$ strains in M9 medium. The values are shown as mean and standard deviation of three biological replicates ($n = 3$) and were analyzed using one-way ANOVA. **, $P < 0.01$; ***, $P < 0.001$; ****, $P < 0.0001$.

capacity of the $\Delta degS$ strain was significantly reduced, while the colonization capacity of the $\Delta degS::degS$ strain was similar to that of the WT strain, and the colonization ability of the $\Delta degS+icdh$ strain was partially restored (Figure 7). However, the colonization ability of $\Delta degS\Delta arcA$ was comparable to that of $\Delta degS$, and the colonization ability of $\Delta degS\Delta arcA::arcA$ was stronger than that of $\Delta degS\Delta arcA$ strain.

Discussion

Aerobic respiration is a major driver of *V. cholerae* proliferation during infection. *V. cholerae* require energy from aerobic respiration for subsequent proliferation and infection (Van Alst and DiRita, 2020). Here, we observed that DegS protease plays a vital role in NADH and ATP levels, growth, and colonization of *V. cholerae*. We propose a model whereby DegS positively regulates ATP and NADH levels to promote the growth of *V. cholerae*, which is in part dependent on the ArcA-ICDH pathway. In addition, there may be other factors (X) involved in the effects of DegS on *V. cholerae* NADH and ATP levels, and growth (Figure 8).

The DegS serine protease is located within the bacterial periplasm. The protein is thought to be involved in initiating the σ^E stress response pathway, where active DegS catalyzes the cleavage of RseA, releasing active σ^E , which activates σ^E -regulated gene expression (Sohn et al., 2007; Chaba et al., 2011). Although σ^E is involved in a variety of biological processes, such as stress response, biofilm formation, and motility (Liang et al., 2021), its relevance to aerobic respiration has remained unclear. Our study reveals that the levels of NADH and ATP, which are key products of

aerobic respiration, decreased upon deletion of *degS* (Figure 2A, B). However, deletion of *rpoE* had little effect on NADH and ATP levels (Figures 3B, C). In addition, qRT-PCR results revealed no statistically significant changes in any of the relevant aerobic respiration genes in the $\Delta rpoE$ strain (Figure 3D). Given these results, we speculate that the effect of DegS on *V. cholerae* NADH and ATP levels is independent of σ^E . This suggests that DegS may have a different pathway than the previous dependence on σ^E .

Further investigating the mechanism by which DegS affects NADH and ATP levels in *V. cholerae*, we observed using RNA-seq that deletion of *degS* mainly inhibits the TCA cycle, carbon metabolism, and pyruvate metabolism (Huang et al., 2019). Meanwhile, qRT-PCR results showed that aerobic respiratory-related genes were altered in the $\Delta degS$ mutant (Figure 3D). Among them, the expression of the *gap* gene, which is a key enzyme involved in glycolysis, was significantly reduced. Expression of the *pckA* gene, which is involved in gluconeogenesis, was also reduced. Notably, the expression of the *icdh* gene, a key gene in the TCA cycle, was significantly reduced. Since the TCA cycle is a major biochemical hub in most heterotrophic organisms, it is essential for aerobic respiration (Brandenburg et al., 2021; Jiang et al., 2023). Therefore, we chose *icdh* to further investigate the mechanism by which DegS affects NADH and ATP levels in *V. cholerae*.

ArcA acts as a response factor in a two-component system to directly or indirectly inhibit the TCA cycle, thereby reshuffling bacterial metabolic pathways and optimizing energy conversion (Gunsalus and Park, 1994; Liu and De Wulf, 2004; Brown et al., 2023). ArcA as a global transcription factor responds to NADH and ATP (Holm et al., 2010). In addition, the $\Delta arcA$ strain of *Salmonella enterica* displays higher levels of NADH (Morales et al., 2013). In

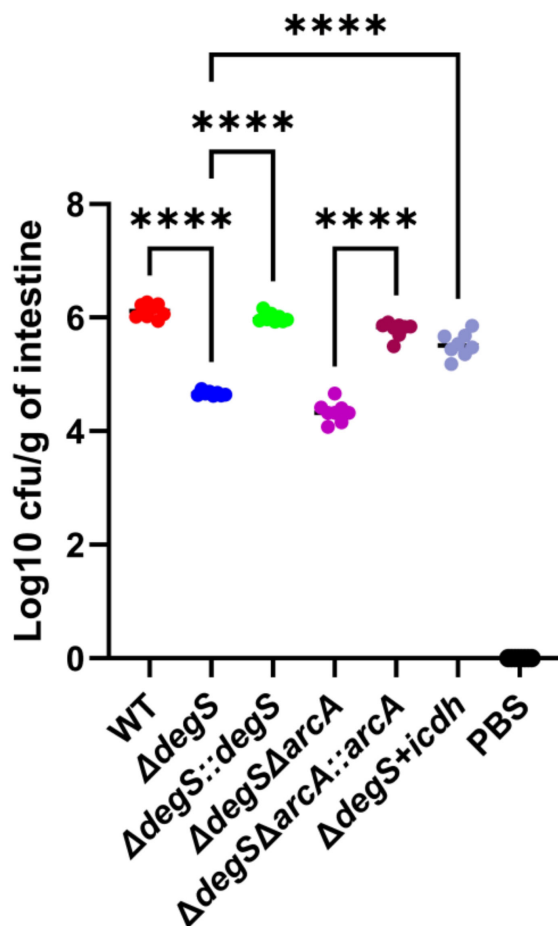


FIGURE 7

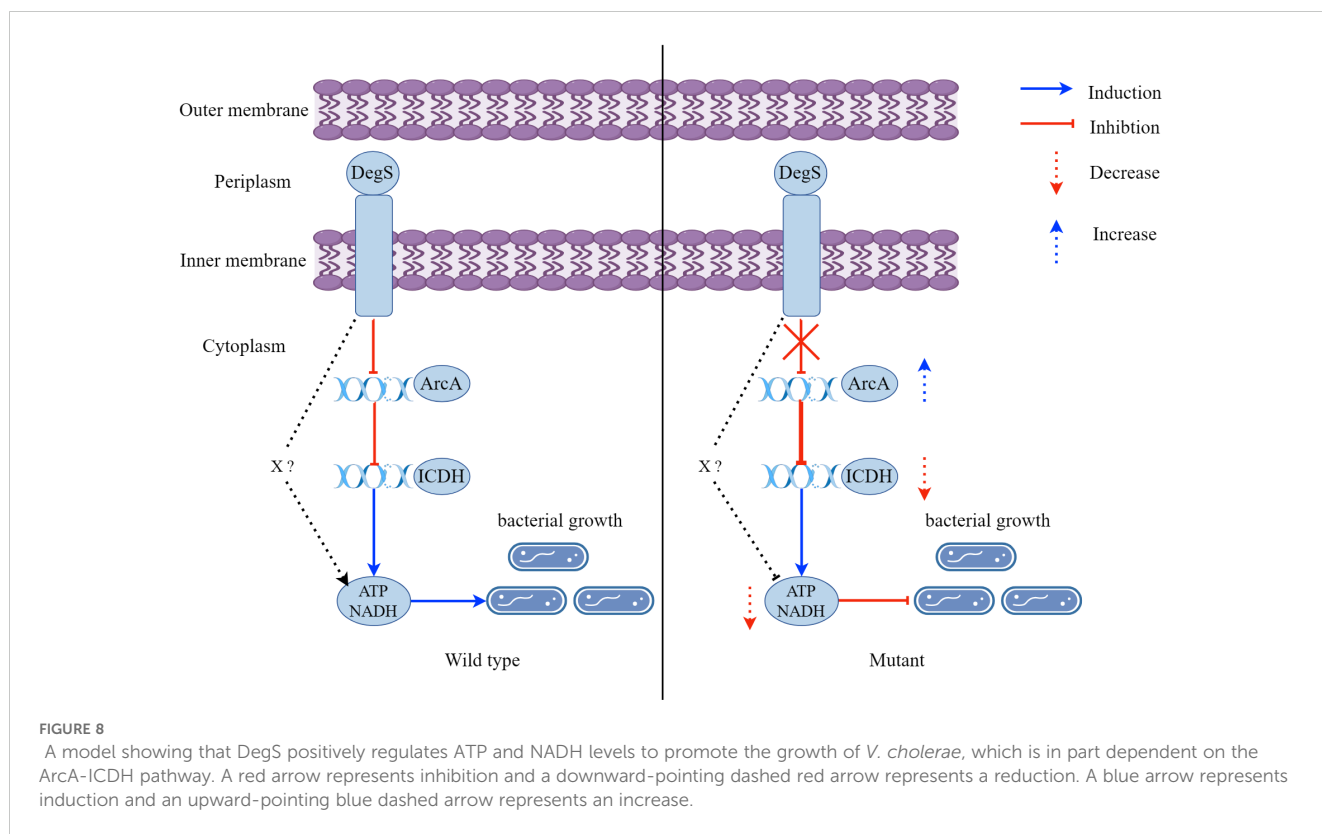
DegS affects *V. cholerae* intestinal colonization. Approximately 10^7 cells of different strains were gavaged into suckling mice. The results obtained after 18 h are expressed as the logarithm of colony-forming units/g intestine (CFU/g; mean \pm SD, $n = 8$). Values were analyzed by one-way ANOVA, ****, $P < 0.0001$.

In this study, we observed that an increase in transcript levels of *arcA* after knockout of *degS* (Figure 4A) and knockout of the *arcA* gene partially restored the low levels of NADH and ATP levels in the $\Delta degS$ strain (Figures 4B, C). At the protein level, western blot experiments revealed no difference in ArcA protein expression in the $\Delta degS$ strain (Figure 4D). Therefore, we speculate that the post-translational modification of ArcA may be involved in the regulation of NADH and ATP by DegS. ArcA can be activated as a transcription factor via phosphorylation to regulate the expression of downstream genes (Yan et al., 2021). Therefore, suspecting that ArcA may play a role in phosphorylation, we constructed a model of dephosphorylation by point mutation ($\Delta degS \Delta arcA::arcA^{D54E}$). Both NADH and ATP levels were lower significantly in the point mutant strain compared to the $\Delta degS \Delta arcA$ strain, but not as much as in the $\Delta degS \Delta arcA::arcA$ strain (Figures 4E, F). Thus, we speculated that DegS affects NADH and ATP levels is partially dependent on ArcA phosphorylation. This phenomenon is similar to the EnvZ/OmpR two-component system in *Klebsiella pneumoniae*, where the $\Delta ompR$ mutant completely loses mucoviscosity compared to the wild-type strain, while the unphosphorylated *ompR*^{D55A} mutant reduces mucoviscosity only

to a lesser extent, suggesting that phosphorylation only partially affects its phenotype (Wang et al., 2023b). Brown et al. show that the conserved metabolic regulator ArcA responds to host-mediated cell envelope damage (Brown et al., 2023). Meanwhile, DegS is a serine protease that mediates the cell envelope stress response, so we hypothesized that they might be linked through the cell envelope stress response pathway.

ICDH is one of the vital rate-limiting enzymes in the TCA cycle (Krebs and Johnson, 1980; Cronan and Laporte, 2005) and its transcription is dependent on ArcA (Chao et al., 1997). In addition, knockout of *icdh* in the TCA cycle results in changes in the central metabolism of *E. coli*, such as a decrease in intracellular NADH and ATP levels and a decrease in the rate of glucose consumption (Kabir and Shimizu, 2004a). In the current study, qRT-PCR showed that DegS positively regulated *icdh*, and ArcA negatively regulated the *icdh* gene (Figure 5A). Overexpression of ICDH partially restored NADH and ATP levels in the $\Delta degS$ strain (Figures 5B, C). Based on these results, we suggest that DegS affects NADH and ATP levels in *V. cholerae* via ArcA, in relation to ICDH.

Bacteria require energy to grow, and a decrease in the energy supply can inhibit their growth (Orellana et al., 2022; Ren et al., 2022).



ATP and NADH are important components of the energy supply and are essential for bacterial growth. Previous studies demonstrated that ArcA affects bacterial NADH levels and growth (Xie et al., 2021; Yan et al., 2021). In addition, deletion of *E. coli icdh* leads to alterations in NADH and ATP levels, thereby affecting specific growth (Kabir and Shimizu, 2004a). Here, we observed that the trends in NADH and ATP levels of the $\Delta degS \Delta arcA$ and $\Delta degS + icdh$ strains in the M9 medium (Figure 6C, D) were consistent with the same growth rate trends in the logarithmic growth phase (Figures 6A, B). Therefore, we propose that DegS regulates *V. cholerae* NADH and ATP levels through the ArcA-ICDH pathway, thereby affecting *V. cholerae* growth. Given that the $\Delta degS \Delta arcA$ strain and the $\Delta degS + icdh$ strain only partially restored the growth rate of $\Delta degS$ in the logarithmic growth phase, NADH and ATP levels were not fully restored in the $\Delta degS + icdh$ strain, we speculate that DegS regulation of *V. cholerae* growth and the levels of ATP and NADH may involve other factors.

Energy is an important driver of bacterial colonization (Chandrashekhara et al., 2018). We observed a highly significantly reduced colonization ability in the $\Delta degS$ mutant, consistent with our previous study (Zou et al., 2023). However, the colonization ability of $\Delta degS \Delta arcA$ was not restored to a certain extent. This result may be due to the fact that *arcA* is required for *V. cholerae* biofilm formation (Xi et al., 2020), which is important for intestinal colonization (Silva and Benitez, 2016). Compared to the $\Delta degS \Delta arcA$ strain, the $\Delta degS + icdh$ strain are directly overexpressing the *icdh* gene and do not involve the knockout of the *arcA* gene, so their colonization ability can be partially restored.

Conclusion

In summary, we demonstrate that deletion of *degS* leads to a decrease in NADH and ATP levels in *V. cholerae* and is independent of σ^E , thus inhibiting *V. cholerae* growth. Furthermore, our findings indicated that DegS may be a prospective mechanism for regulating ICDH expression through ArcA. These findings enhance the knowledge of the biological functions of DegS and offer new perspectives on the regulation of NADH and ATP levels in *V. cholerae*. The role of DegS in ICDH regulation through ArcA independent of σ^E needs to be further investigated.

Data availability statement

The datasets presented in this study can be found in online repositories. The names of the repository/repositories and accession number(s) can be found in the article/Supplementary Material.

Ethics statement

The animal study was approved by the Ethics Committee of Zunyi Medical University (No. ZMU21-2301-069). The study was conducted in accordance with the local legislation and institutional requirements.

Author contributions

JZ: Data curation, Formal analysis, Investigation, Validation, Visualization, Writing – original draft. XH: Data curation, Formal analysis, Investigation, Validation, Visualization, Writing – original draft. QL: Data curation, Formal analysis, Investigation, Validation, Visualization, Writing – original draft. FR: Data curation, Formal analysis, Methodology, Writing – review & editing. HH: Data curation, Formal analysis, Methodology, Writing – original draft. JY: Formal analysis, Investigation, Writing – review & editing. KW: Data curation, Formal analysis, Methodology, Writing – review & editing. YH: Data curation, Formal analysis, Methodology, Writing – review & editing. JH: Conceptualization, Data curation, Funding acquisition, Project administration, Writing – review & editing. XM: Conceptualization, Data curation, Funding acquisition, Project administration, Writing – review & editing.

Funding

The author(s) declare that financial support was received for the research, authorship, and/or publication of this article. This work was supported by grants from the National Natural Science Foundation of China (No. 32060035, 82360397), the Research and Talent Training Project of Guizhou Moutai Hospital (MTyk 2022-08).

References

- Ades, S. E., Connolly, L. E., Alba, B. M., and Gross, C. A. (1999). The Escherichia coli sigma(E)-dependent extracytoplasmic stress response is controlled by the regulated proteolysis of an anti-sigma factor. *Genes Dev.* 13, 2449–2461. doi: 10.1101/gad.13.18.2449
- Basan, M., Hui, S., and Williamson, J. R. (2017). ArcA overexpression induces fermentation and results in enhanced growth rates of E. coli. *Sci. Rep.* 7, 11866. doi: 10.1038/s41598-017-12144-6
- Brandenburg, F., Theodosiou, E., Bertelmann, C., Grund, M., Klähn, S., Schmid, A., et al. (2021). Trans-4-hydroxy-L-proline production by the cyanobacterium *Synechocystis* sp. PCC 6803. *Metab. Eng. Commun.* 12, e00155. doi: 10.1016/j.mec.2020.e00155
- Brown, A. N., Anderson, M. T., Smith, S. N., Bachman, M. A., and Mobley, H. L. T. (2023). Conserved metabolic regulator ArcA responds to oxygen availability, iron limitation, and cell envelope perturbations during bacteremia. *MBio* 14, e0144823. doi: 10.1128/mbio.01448-23
- Bueno, E., Sit, B., Waldor, M. K., and Cava, F. (2020). Genetic dissection of the fermentative and respiratory contributions supporting vibrio cholerae hypoxic growth. *J. Bacteriology* 202, e00243-20. doi: 10.1128/JB.00243-20
- Chaba, R., Alba, B. M., Guo, M. S., Sohn, J., Ahuja, N., Sauer, R. T., et al. (2011). Signal integration by DegS and RseB governs the σ^E -mediated envelope stress response in Escherichia coli. *Proc. Natl. Acad. Sci. U.S.A.* 108, 2106–2111. doi: 10.1073/pnas.1019277108
- Chandrasekhar, K., Srivastava, V., Hwang, S., Jeon, B., Ryu, S., and Rajashekhara, G. (2018). Transducer-like protein in campylobacter jejuni with a role in mediating chemotaxis to iron and phosphate. *Front. Microbiol.* 9. doi: 10.3389/fmicb.2018.02674
- Chao, G., Shen, J., Tseng, C. P., Park, S. J., and Gunsalus, R. P. (1997). Aerobic regulation of isocitrate dehydrogenase gene (icd) expression in Escherichia coli by the arcA and fnr gene products. *J. Bacteriology* 179, 4299–4304. doi: 10.1128/jb.179.13.4299-4304.1997
- Cronan, J. E., and Laporte, D. (2005). Tricarboxylic acid cycle and glyoxylate bypass. *EcoSal Plus* 1. doi: 10.1128/ecosalplus.3.5.2
- D'Oria, A., Jing, L., Arkoun, M., Pluchon, S., Pateyron, S., Trouverie, J., et al. (2022). Transcriptomic, Metabolomic and Ionomic Analyses Reveal Early Modulation of Leaf Mineral Content in Brassica napus under Mild or Severe Drought. *Int. J. Mol. Sci.* 23, 781. doi: 10.3390/ijms23020781

Conflict of interest

The authors declare that they have no competing financial interests or personal relationships that influenced the work reported in this paper.

Publisher's note

All claims expressed in this article are solely those of the authors and do not necessarily represent those of their affiliated organizations, or those of the publisher, the editors and the reviewers. Any product that may be evaluated in this article, or claim that may be made by its manufacturer, is not guaranteed or endorsed by the publisher.

Supplementary material

The Supplementary Material for this article can be found online at: <https://www.frontiersin.org/articles/10.3389/fcimb.2024.1482919/full#supplementary-material>

de Regt, A. K., Baker, T. A., and Sauer, R. T. (2015). Steric clashes with bound OMP peptides activate the DegS stress-response protease. *Proc. Natl. Acad. Sci. U.S.A.* 112, 3326–3331. doi: 10.1073/pnas.1502372112

Fan, F., Liu, Z., Jabeen, N., Birdwell, L. D., Zhu, J., and Kan, B. (2014). Enhanced interaction of Vibrio cholerae virulence regulators TcpP and ToxR under oxygen-limiting conditions. *Infect. Immun.* 82, 1676–1682. doi: 10.1128/IAI.01377-13

Fisher, C. L., and Pei, G. K. (1997). Modification of a PCR-based site-directed mutagenesis method. *Biotechniques* 23, 570–574. doi: 10.2144/97234bm01

Gessner, P., Lum, J., and Frenguelli, B. G. (2023). The mammalian purine salvage pathway as an exploitable route for cerebral bioenergetic support after brain injury. *Neuropharmacology* 224, 109370. doi: 10.1016/j.neuropharm.2022.109370

Gunsalus, R. P., and Park, S. J. (1994). Aerobic-anaerobic gene regulation in Escherichia coli: control by the ArcAB and Fnr regulons. *Res. Microbiol.* 145, 437–450. doi: 10.1016/0923-2508(94)90092-2

Harris, J. B., LaRocque, R. C., Qadri, F., Ryan, E. T., and Calderwood, S. B. (2012). Cholera. *Lancet* 379, 2466–2476. doi: 10.1016/S0140-6736(12)60436-X

Hatem, E., Berthonaud, V., Dardalhon, M., Lagniel, G., Baudouin-Cornu, P., Huang, M.-E., et al. (2014). Glutathione is essential to preserve nuclear function and cell survival under oxidative stress. *Free Radic. Biol. Med.* 67, 103–114. doi: 10.1016/j.freeradbiomed.2013.10.807

Hill, N. S., Buske, P. J., Shi, Y., and Levin, P. A. (2013). A moonlighting enzyme links Escherichia coli cell size with central metabolism. *PLoS Genet.* 9, e1003663. doi: 10.1371/journal.pgen.1003663

Holm, A. K., Blank, L. M., Oldiges, M., Schmid, A., Solem, C., Jensen, P. R., et al. (2010). Metabolic and transcriptional response to cofactor perturbations in Escherichia coli. *J. Biol. Chem.* 285, 17498–17506. doi: 10.1074/jbc.M109.095570

Huang, J., Chen, Y., Chen, J., Liu, C., Zhang, T., Luo, S., et al. (2019). Exploration of the effects of a degS mutant on the growth of Vibrio cholerae and the global regulatory function of degS by RNA sequencing. *PeerJ* 7, e7959. doi: 10.7717/peerj.7959

Janet-Maitre, M., Pont, S., Masson, F. M., Sleiman, S., Trouillon, J., Robert-Genthon, M., et al. (2023). Genome-wide screen in human plasma identifies multifaceted complement evasion of Pseudomonas aeruginosa. *PLoS Pathog.* 19, e1011023. doi: 10.1371/journal.ppat.1011023

Jeon, Y., Lee, Y. S., Han, J. S., Kim, J. B., and Hwang, D. S. (2001). Multimerization of phosphorylated and non-phosphorylated ArcA is necessary for the response regulator

- function of the Arc two-component signal transduction system. *J. Biol. Chem.* 276, 40873–40879. doi: 10.1074/jbc.M104855200
- Jiang, P.-C., Fan, J., Zhang, C.-D., Bai, M.-H., Sun, Q.-Q., Chen, Q.-P., et al. (2023). Unraveling colorectal cancer and pan-cancer immune heterogeneity and synthetic therapy response using cuproptosis and hypoxia regulators by multi-omic analysis and experimental validation. *Int. J. Biol. Sci.* 19, 3526–3543. doi: 10.7150/ijbs.84781
- Jones, S. A., Chowdhury, F. Z., Fabich, A. J., Anderson, A., Schreiner, D. M., House, A. L., et al. (2007). Respiration of *Escherichia coli* in the mouse intestine. *Infect. Immun.* 75, 4891–4899. doi: 10.1128/IAI.00484-07
- Kabir, M. M., and Shimizu, K. (2004a). Metabolic regulation analysis of *icd*-gene knockout *Escherichia coli* based on 2D electrophoresis with MALDI-TOF mass spectrometry and enzyme activity measurements. *Appl. Microbiol. Biotechnol.* 65, 84–96. doi: 10.1007/s00253-004-1627-1
- Kiiyukia, C., Kawakami, H., and Hashimoto, H. (1993). Effect of sodium chloride, pH and organic nutrients on the motility of *Vibrio cholerae* non-01. *Microbios* 73, 249–255.
- Kovač, U., Žužek, Z., Raspor Dall'Olio, L., Pohar, K., Ihan, A., Moškon, M., et al. (2021). *Escherichia coli* affects expression of circadian clock genes in human hepatoma cells. *Microorganisms* 9, 869. doi: 10.3390/microorganisms9040869
- Krebs, H. A., and Johnson, W. A. (1980). The role of citric acid in intermediate metabolism in animal tissues. *FEBS Lett.* 117 Suppl, K1–10. doi: 10.4159/harvard.9780674366701.c143
- Liang, H., Zhang, Y., Wang, S., and Gao, H. (2021). Mutual interplay between ArcA and σ^E orchestrates envelope stress response in *Shewanella oneidensis*. *Environ. Microbiol.* 23, 652–668. doi: 10.1111/1462-2920.15060
- Liu, X., and De Wulf, P. (2004). Probing the ArcA-P modulon of *Escherichia coli* by whole genome transcriptional analysis and sequence recognition profiling. *J. Biol. Chem.* 279, 12588–12597. doi: 10.1074/jbc.M313454200
- Livak, K. J., and Schmittgen, T. D. (2001). Analysis of relative gene expression data using real-time quantitative PCR and the 2(-Delta Delta C(T)) Method. *Methods* 25, 402–408. doi: 10.1006/meth.2001.1262
- Luo, P., Su, T., Hu, C., and Ren, C. (2011). A novel and simple PCR walking method for rapid acquisition of long DNA sequence flanking a known site in microbial genome. *Mol. Biotechnol.* 47, 220–228. doi: 10.1007/s12033-010-9332-z
- Lushchak, V. I. (2012). Glutathione homeostasis and functions: potential targets for medical interventions. *J. Amino Acids* 2012, 736837. doi: 10.1155/2012/736837
- MacLean, A., Legendre, F., and Appanna, V. D. (2023). The tricarboxylic acid (TCA) cycle: a malleable metabolic network to counter cellular stress. *Crit. Rev. Biochem. Mol. Biol.* 58, 81–97. doi: 10.1080/10409238.2023.2201945
- Medrano, A. I., DiRita, V. J., Castillo, G., and Sanchez, J. (1999). Transient transcriptional activation of the *Vibrio cholerae* El Tor virulence regulator *toxT* in response to culture conditions. *Infect. Immun.* 67, 2178–2183. doi: 10.1128/IAI.67.5.2178-2183.1999
- Morales, E. H., Collao, B., Desai, P. T., Calderón, I. L., Gil, F., Luraschi, R., et al. (2013). Probing the ArcA regulon under aerobic/ROS conditions in *Salmonella enterica* serovar Typhimurium. *BMC Genomics* 14, 626. doi: 10.1186/1471-2164-14-626
- Orellana, C., Castellano, G., Escanilla, J., and Parraguez, V. H. (2022). Use of fecal indices as a non-invasive tool for ruminal activity evaluation in extensive grazing sheep. *Anim. (Basel)* 12, 974. doi: 10.3390/ani12080974
- Park, D. M., Akhtar, M. S., Ansari, A. Z., Landick, R., and Kiley, P. J. (2013). The bacterial response regulator ArcA uses a diverse binding site architecture to regulate carbon oxidation globally. *PLoS Genet.* 9, e1003839. doi: 10.1371/journal.pgen.1003839
- Reen, F. J., Almagro-Moreno, S., Ussery, D., and Boyd, E. F. (2006). The genomic code: inferring Vibrionaceae niche specialization. *Nat. Rev. Microbiol.* 4, 697–704. doi: 10.1038/nrmicro1476
- Ren, S., Wang, W., Jia, M., An, L., Tang, T., and Liu, X. (2022). Proteomic Analysis of the Antibacterial Effect of Improved Dian Dao San against *Propionibacterium acnes*. *Evid Based Complement Alternat Med.* 2022, 3855702. doi: 10.1155/2022/3855702
- Schurig-Briccio, L. A., Parraga Solorzano, P. K., Lencina, A. M., Radin, J. N., Chen, G. Y., Sauer, J.-D., et al. (2020). Role of respiratory NADH oxidation in the regulation of *Staphylococcus aureus* virulence. *EMBO Rep.* 21, e45832. doi: 10.15252/embr.201845832
- Silva, A. J., and Benitez, J. A. (2016). *Vibrio cholerae* biofilms and cholera pathogenesis. *PLoS Negl. Trop. Dis.* 10, e0004330. doi: 10.1371/journal.pntd.0004330
- Sohn, J., Grant, R. A., and Sauer, R. T. (2007). Allosteric activation of DegS, a stress sensor PDZ protease. *Cell* 131, 572–583. doi: 10.1016/j.cell.2007.08.044
- Sperber, A. M., and Herman, J. K. (2017). Metabolism shapes the cell. *J. Bacteriology* 199, e00039–17. doi: 10.1128/JB.00039-17
- Van Alst, A. J., Demey, L. M., and DiRita, V. J. (2022). *Vibrio cholerae* requires oxidative respiration through the *bd-I* and *cbb3* oxidases for intestinal proliferation. *PLoS Pathog.* 18, e1010102. doi: 10.1371/journal.ppat.1010102
- Van Alst, A. J., and DiRita, V. J. (2020). Aerobic Metabolism in *Vibrio cholerae* Is Required for Population Expansion during Infection. *MBio* 11, e01989–20. doi: 10.1128/mBio.01989-20
- Wang, L., Huang, X., Jin, Q., Tang, J., Zhang, H., Zhang, J.-R., et al. (2023b). Two-Component Response Regulator OmpR Regulates Mucoviscosity through Energy Metabolism in *Klebsiella pneumoniae*. *Microbiol. Spectr.* 11, e0054423. doi: 10.1128/spectrum.00544-23
- Wang, K., Lu, H., Zou, M., Wang, G., Zhao, J., Huang, X., et al. (2023a). DegS protease regulates antioxidant capacity and adaptability to oxidative stress environment in *Vibrio cholerae*. *Front. Cell Infect. Microbiol.* 13. doi: 10.3389/fcimb.2023.1290508
- Wang, Z., Sun, J., Xia, T., Liu, Y., Fu, J., Lo, Y. K., et al. (2018). Proteomic delineation of the arcA regulon in *Salmonella typhimurium* during anaerobiosis. *Mol. Cell Proteomics* 17, 1937–1947. doi: 10.1074/mcp.RA117.000563
- Weart, R. B., Lee, A. H., Chien, A.-C., Haeusser, D. P., Hill, N. S., and Levin, P. A. (2007). A metabolic sensor governing cell size in bacteria. *Cell* 130, 335–347. doi: 10.1016/j.cell.2007.05.043
- Wu, R., Zhao, M., Li, J., Gao, H., Kan, B., and Liang, W. (2015). Direct regulation of the natural competence regulator gene *tfoX* by cyclic AMP (cAMP) and cAMP receptor protein (CRP) in *Vibrios*. *Sci. Rep.* 5, 14921. doi: 10.1038/srep14921
- Xi, D., Yang, S., Liu, Q., Li, Y., Li, Y., Yan, J., et al. (2020). The response regulator ArcA enhances biofilm formation in the *vpsT* manner under the anaerobic condition in *Vibrio cholerae*. *Microb. Pathog.* 144, 104197. doi: 10.1016/j.micpath.2020.104197
- Xia, Y., Cebrián, R., Xu, C., Ad, J., Wu, W., and Kuipers, O. P. (2021). Elucidating the mechanism by which synthetic helper peptides sensitize *Pseudomonas aeruginosa* to multiple antibiotics. *PLoS Pathog.* 17, e1009909. doi: 10.1371/journal.ppat.1009909
- Xie, P., Wang, J., Liang, H., and Gao, H. (2021). *Shewanella oneidensis* arcA Mutation Impairs Aerobic Growth Mainly by Compromising Translation. *Life (Basel)* 11, 926. doi: 10.3390/life11090926
- Yan, J., Li, Y., Guo, X., Wang, X., Liu, F., Li, A., et al. (2021). The effect of ArcA on the growth, motility, biofilm formation, and virulence of *Plesiomonas shigelloides*. *BMC Microbiol.* 21, 266. doi: 10.1186/s12866-021-02322-y
- Zhang, C., Liu, C., Wu, H., Wang, J., Sun, Y., Liu, R., et al. (2021). Global analysis the potential medicinal substances of shuangxia decoction and the process *in vivo* via mass spectrometry technology. *Front. Pharmacol.* 12. doi: 10.3389/fphar.2021.654807
- Zou, M., Wang, K., Zhao, J., Lu, H., Yang, H., Huang, M., et al. (2023). DegS protease regulates the motility, chemotaxis, and colonization of *Vibrio cholerae*. *Front. Microbiol.* 14. doi: 10.3389/fmicb.2023.1159986